Interdisciplinary Information Sciences, Vol. 2, No. 2, pp. 111–123 (1996)

Correlated-Walks Seen from the Viewpoint of Information Geometry

Tsunehiro OBATA* and Hiroaki HARA**

**Department of Electrical Engineering, Gunma National College of Technology, Toriba-machi, Maebashi 371, Japan*
***Graduate School of Information Science, Tohoku University, Aoba-ku, Sendai 980, Japan*

Received January 5, 1996; final version accepted June 6, 1996

A statistical manifold associated with a correlated walk (CW) model is examined by noticing a non-Riemannian curvature, called the α-curvature, as well as the Riemann curvature. Dynamical characteristics of the Riemann curvature and the α-curvature are discussed to have a close relation to the stability of the CW system. The statistical manifold is also found to be asymptotically flat in the meaning of the $\alpha(=1)$-curvature, and also the jump probabilities characterizing the CW model is shown to have relation to a symmetry of the statistical manifold. Moreover a forecast is given about the statistical manifolds of n-step correlated-walk models and nonlinear models, and also such time-developing statistical manifolds are shown to be very analogous to the geometrical structure of Newton-Cartan theory of gravity.

1 Introduction

Many researchers tried to introduce the notion of distance into the state spaces of equilibrium thermodynamical systems such as the $T - \mu$ space (Ruppeiner (1979, 1995), Janyszek (1986, 1990), Janyszek and Mrugala (1989, 1990), Ruppeiner and Davis (1990), Ginoza (1993)). They had an interest mainly in the metric tensor and the Riemann curvature. A noteworthy result is that the Riemann scalar curvature largely increases near phase transition points. This fact led some researchers to interpret the Riemann scalar curvature as a measure of unstability or fluctuation.

Recently we proposed two differential-geometrical approaches to the time development of non-equilibrium systems (Obata, Hara and Endo (1992)). One approach depicts the time development by the motion of a point in a statistical manifold, and the other one by the motion of a statistical manifold itself.

The former approach showed that the Uhlenbeck-Ornstein process is a geodesic motion in the statistical manifold of negative constant curvature. This viewpoint has been further developed by other researchers (Nakamura (1993), Fujiwara and Amari (1993)).

On the other hand the latter approach showed that a D-dimensional random walk (RW) accompanies the expansion of a 2D-dimensional sphere. As a step time N increases, the sphere expands with the radius of $2\sqrt{N}$ from the singular state of zero radius to the flat sphere of infinite radius. In other words the curvature tensor fades away as $1/N$. We regarded this decrease behavior of the curvature tensor as a geometrical representation of approach from an initial unstable state to a stable equilibrium state. This interpretation is consistent with the results for equilibrium systems (Ruppeiner (1979, 1995), Janyszek (1986, 1990), Janyszek and Mrugala (1989, 1990), Ruppeiner and Davis (1990), Ginoza (1993)): the curvature for stable equilibrium systems becomes small.

In successive papers (Obata, Hara and Endo (1994a, 1994b)) we extended the latter approach from the RW model to a correlated walk (CW) model. The statistical manifold associated with the CW model is spanned by two parameters representing the jump probabilities of the CW model. We there studied the Riemann scalar curvature of the CW manifold, and showed that the time development of the CW produces inhomogeneous expansion from a spherical surface of $R = 1/2$ to a saddle surface of $R = -1$ through an era of violent oscillation. Such behavior of the Riemann scalar curvature was shown to be well understood by the terms of 'stability' and 'order parameter' of stochastic processes.

In the present paper we examine the α-curvature of the CW model as well as the Riemann curvature. The statistical manifold is also found to be asymptotically flat in the meaning of the $\alpha(=1)$-curvature. This geometrical characteristic of the CW model is common to equilibrium thermodynamical systems. Moreover the jump probabilities characterizing the CW model are shown to be a preferred coordinate system in the CW manifold. Finally on the results about the RW model and the CW model a forecast is given about the statistical manifolds of n-step correlated-walk models and nonlinear models, and also such time-developing statistical manifolds are shown to be very analogous to the geometrical structure of Newton-Cartan theory of gravity.

2 Statistical manifolds

We here give a brief summary of statistical manifold (Amari (1985)). In particular, the decomposition of the 2-dimensional α-curvature into three scalars will play an important role in the next section.

Note that we follow the Misner-Thorn-Wheeler convention for the notation of connection coefficients and curvature tensors (Misner, Thorne and Wheeler (1973)).

Let $S = \{p(x, \theta)\}$ be a parameterized family of probability density functions $p(x, \theta)$, where x is a random variable and $\theta = (\theta^1, \cdots, \theta^n)$ is a n-dimensional parameter. An element of S, that is, a probability density function is specified by the parameter θ. In other words the parameter θ is a coordinate system on S. At every point there exists a tangent vector space T_θ, that is represented as a linear combination of n coordinate-differential operators $\partial_i = \partial/\partial\theta^i$, $i = 1, \cdots, n$:

$$T_\theta \equiv \{A \mid A = A^i \partial_i\}. \tag{1}$$

In the statistical manifold S, one can construct another vector space, called the 1-representation of the T_θ, that is isomorphic to the tangent vector space T_θ. It is spanned with n partial derivatives $\partial_i l(x, \theta)$ of the function $l(x, \theta) \equiv \ln p(x, \theta)$:

$$T_\theta^{(1)} \equiv \{A(x) \mid A(x) = A^i \partial_i l(x, \theta)\}. \tag{2}$$

For any random variable $A(x)$, we have $E[A(x)] = 0$. The symbol $E[\,\cdot\,]$ is the expectation with respect to the distribution $p(x, \theta)$.

The inner product of two tangent vectors is defined by

$$g(A, B) \equiv E[A(x)B(x)] = g_{ij} A^i B^j \tag{3}$$

with

$$g_{ij}(\theta) \equiv E[\partial_i l(x, \theta) \partial_j l(x, \theta)] = -E[\partial_i \partial_j l(x, \theta)]. \tag{4}$$

The last equality is due to the normalization condition of probability. The inner product is invariant under the transformation of the coordinate θ and also under the transformation of the random variable x.

For a function f and a tangent vector A, we can define the directional derivative $\nabla_A f$ of f toward A by $A(f)$. The derivative satisfies the linearity condition and the Leibnitz condition.

For a vector field B and a tangent vector A, one can introduce a directional derivative $\nabla_A B$ of B toward A. If one require the directional derivative to be invariant not only under the transformation of the coordinate θ but also under the random variable, the derivative is unique except for a constant α. The derivative $\nabla_A B$ is introduced through the inner product

$$g(\nabla_A B, C) \equiv E\left[\left(ABl + \frac{1-\alpha}{2} AlBl\right)Cl\right]. \tag{5}$$

The components

$$\Gamma_{ijk} \equiv g(\nabla_{\partial_k} \partial_j, \partial_i) = E\left[\left(\partial_j \partial_k l + \frac{1-\alpha}{2} \partial_j l \partial_k l\right)\partial_i l\right] \tag{6}$$

are called the α-connection coefficients.

If necessary, we express a value of α by superfix such as $\nabla^{(\alpha)}$, $\Gamma^{(\alpha)}_{ijk}, \cdots$. In case of $\alpha = 0$, the α connection reduces to the Levi-Civita connection:

$$\Gamma^{(0)}_{ijk} = 1/2(\partial_k g_{ij} + \partial_j g_{ik} - \partial_i g_{jk}). \tag{7}$$

It is often useful to decompose the α-connection as follows:

$$\Gamma_{ijk} = \Gamma^{(1)}_{ijk} + \frac{1-\alpha}{2} T_{ijk} = \Gamma^{(0)}_{ijk} - \frac{\alpha}{2} T_{ijk} \tag{8}$$

with

$$T_{ijk} = E[\partial_i l \partial_j l \partial_k l] = -E[\partial_i \partial_j \partial_k l] - E[(\partial_i l)(\partial_j \partial_k l) + (\partial_j l)(\partial_k \partial_i l) + (\partial_k l)(\partial_i \partial_j l)]. \tag{9}$$

The tensor T is completely symmetric. The last equality is due to the normalization condition of probability.

For three vector fields A, B, and C, the successive derivative $\nabla_A \nabla_B C$ is not equal to the inverse-ordered derivative $\nabla_B \nabla_A C$ in general. An useful measure of the non-commutativity is obtained by subtracting from the difference vector $[\nabla_A, \nabla_B]C$ the contribution due to the non-commutativity of A and B:

$$R(A, B, C) \equiv R(A, B)C = [\nabla_A, \nabla_B]C - \partial_{[\nabla_A, \nabla_B]} C. \tag{10}$$

Its coordinate components are

$$R(\partial_k, \partial_l, \partial_j) = R(\partial_k, \partial_l)\partial_j = [\nabla_{\partial_k}, \nabla_{\partial_l}]\partial_j = R^i_{jkl}\partial_i \tag{11}$$

with

$$R^i_{jkl} \equiv \partial_k \Gamma^i_{jl} - \partial_l \Gamma^i_{jk} + \Gamma^i_{mk}\Gamma^m_{jl} - \Gamma^i_{ml}\Gamma^m_{jk}. \tag{12}$$

The covariant components R_{ijkl} are given by

$$R_{ijkl} = g_{im}R^m_{jkl} = \partial_k \Gamma_{ijl} - \partial_l \Gamma_{ijk} - (\Gamma_{mik} + \alpha T_{\mathrm{mik}})\Gamma^m_{jl} + (\Gamma_{mil} + \alpha T_{mil})\Gamma^m_{jk}. \tag{13}$$

Substitution of eq. (8) yields

$$R_{ijkl} = R^{(0)}_{ijkl} - \frac{\alpha}{2}(\nabla^{(0)}_k T_{ijl} - \nabla^{(0)}_l T_{ijk}) + \frac{\alpha^2}{4} g^{mn}(T_{mik}T_{njl} - T_{mil}T_{njk}). \tag{14}$$

The α-curvature tensor is antisymmetric in the last two indices k and l. As for the first two indices i and j, formula (14) gives an useful decomposition. The α^0 term, that is, the Riemann curvature tensor is antisymmetric. The α^1 term is symmetric. The α^2 term is antisymmetric. In other words, the odd-order term in α is symmetric and the even-order terms are antisymmetric.

Finally we consider algebraic properties of the 2-dimensional α-curvature tensor. It is convenient to introduce the 2-dimensional completely-antisymmetric tensor η^{ij} ($\eta^{12} = \sqrt{det[g^{ab}]}$). The right-dual operation on the 2-dimensional α-curvature then produces a second rank tensor:

$$R^*_{ij} \equiv R_{ijkl}\eta^{kl}/2! \tag{15}$$

The right-dual tensor is equivalent to the α-curvature tensor. Decompose the right-dual tensor into the antisymmetric tensor $R^*_{[ij]}$ and the symmetric tensor $R^*_{(ij)}$. The antisymmetric tensor is equivalent to the double-dual scalar of the α-curvature tensor:

$$^*R^* \equiv \eta^{ij}/2! R^*_{[ij]}. \tag{16}$$

The symmetric tensor $R^*_{(ij)}$ have two eigenvalues:

$$\left.\begin{matrix} R_1 \\ R_2 \end{matrix}\right\} = \frac{1}{2}\{Trace[R^*_{(mn)}] \pm \sqrt{(Trace[R^*_{(mn)}])^2 - 4det[R^*_{(mn)}]/det[g_{mn}]}\}. \tag{17}$$

Therefore if and only if the three invariants $^*R^*$, R_1, R_2 are zero, the 2-dimensional manifold is α-flat. A scalar curvature is usually defined by

$$R \equiv g^{ik}g^{jl}R_{ijkl}. \tag{18}$$

This scalar is equal to 2 times the double-dual:

$$R = 2^*R^*. \tag{19}$$

This relation is obtained as follows: Choose a local Descartes coordinate system and we then have $2^*R^* = \eta^{ij}R_{ijkl}\eta^{kl}/2 = \eta^{ij}(R_{ij12} - R_{ij21})/2 = \eta^{ij}R_{ij12} = R_{1212} - R_{2112}$ and $R = g^{ik}g^{jl}R_{ijkl} = g^{ik}(R_{i1k1} + R_{i2k2}) = R_{1212} + R_{2121} = R_{1212} - R_{2112}$.

3 A statistical manifold associated with a CW model

Our interest is in the statistical manifolds associated with correlated walks. We here treat a simple CW model proposed by Fujita et al (Fujita (1986)). First we review the CW model.

3.1 CW model

Suppose that a walker moves along a linear lattice of infinite extension right or left with given jump probabilities, which depend on the direction of the previous step. The right and left steps are called steps of type 1 and 2, respectively. If the last step is of type j, the probabilities of stepping right or left are denoted by p_j and q_j, with the normalization condition

$$p_j + q_j = 1, \quad (j = 1, 2). \tag{20}$$

The definition of the step probabilities are shown schematically in figure 1, where the steps in question are indicated by full arrows, and the last steps by broken arrows. The dynamics of the walker with correlated steps can also be represented in a square lattice. [See figure 2]. The walker's moves towards the left on the linear lattice correspond to the upward moves of an object on the square lattice.

Let $P_j(X, Y)$ be the probabilities of the object arriving at the site (X, Y) with step-type j after N units of time. The probability of the object arriving at (X, Y) from any direction is

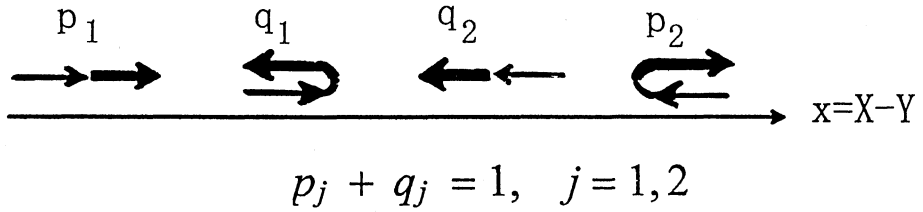

Fig. 1. The definition of step probabilities with correlation.

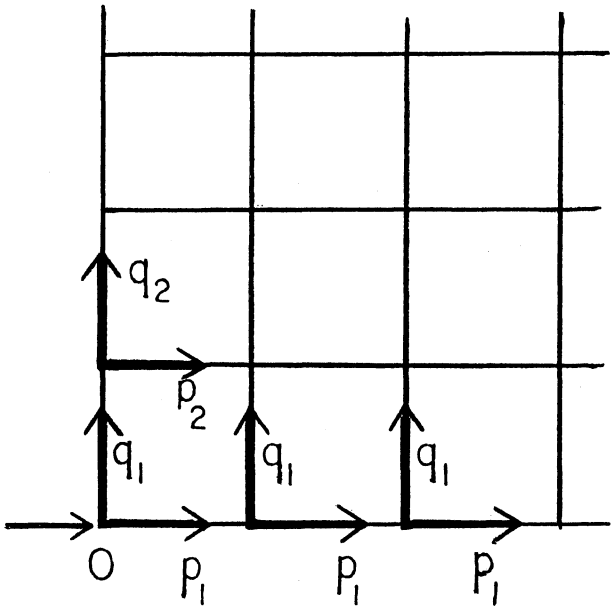

Fig. 2. Step probabilities with correlation can be read by drawing paths in the X-Y lattice. (This figure is cited from ref. [15]).

$$P(X, Y) = P_1(X, Y) + P_2(X, Y). \tag{21}$$

Because of $X+Y=N$, we can regard Ps as functions of X and N. The new function is denoted by Q: $Q_j(X, N) = P_j(X, Y)$, $Q(X, N) = P(X, Y)$. Consideration of two successive steps yields the following relatons for P_j or Q_j:

$$\begin{aligned} Q_1(X, N) &= p_1 Q_1(X-1, N-1) + p_2 Q_2(X-1, N-1), \quad (a) \\ Q_2(X, N) &= q_1 Q_1(X, N-1) + q_2 Q_2(X, N-1), \quad (b) \end{aligned} \tag{22}$$

These are time-development equations for $Q_j(X, N)$.

The basic difference equations (22) were exactly solved under the initial condition of $Q_1(0, 0) = 1$ and $Q_2(0, 0) = 0$ by Chen, Fujia, Okamura and others (See references cited in Fujita (1986)). For other initial conditions one can solve the basic difference equation through the same technique. Those exact solutions, however, are unnecessary in the following.

3.2 A method of numerical analysis of statistical manifolds

Let S be a set of the probability functions $Q(X, N)$ parameterized by the jump probabilities p_j and q_j:

$$S \equiv \{Q(X, N) | 0 < p_1 < 1, 0 < q_2 < 1\}. \tag{23}$$

Because of the normalization condition (20), each function $Q(X, N)$ in S is specified by a 2-dimensional parameter $\theta = (\theta^1, \theta^2)$ such as $\theta = (p_1, q_2)$.

In a standard numerical method of calculating the α-curvature one substitute an exact solution for $Q(X, N)$ into formulas (6), (9) and (13). We performed the numerical calculation in the quadruple precision of 16 bytes. But as the calculation involves alternating series of extremely large terms for $p_1 > p_2$ and large N, we could not obtain reliable results in such cases. Some calculations terminated before $N = 100$. To evade the problem, we

successively solved the basic difference equations (22) and their derivatives step by step. We use the coordinate system (p_1, q_2) for a while. The coordinate system produces the first derivatives (four equations)

$$\frac{\partial Q_1(X,N)}{\partial p_1} = Q_1(X-1,N-1) + p_1\frac{\partial Q_1(X-1,N-1)}{\partial p_1} + p_2\frac{\partial Q_2(X-1,N-1)}{\partial p_1},\cdots \tag{24}$$

and the second derivatives (six equations)

$$\frac{\partial^2 Q_1(X,N)}{\partial p_1 \partial p_1} = 2\frac{\partial Q_1(X-1,N-1)}{\partial p_1} + p_1\frac{\partial^2 Q_1(X-1,N-1)}{\partial p_1 \partial p_1} + p_2\frac{\partial^2 Q_2(X-1,N-1)}{\partial p_1 \partial p_1},\cdots \tag{25}$$

Iterative calculation of the basic difference equations (22), the first derivatives (24) and the second derivatives (25) gives the α-curvature at each step N through formula (13). Note that the third derivatives of the $Q(X, N)$ in the first term $\partial_k \Gamma_{ijl}$ cancel those in the second term $\partial_l \Gamma_{ijk}$.

3.3 α-curvature at $N = 0, 1, 2$

It is possible to analyze the statistical manifold at $N = 0, 1, 2$ without relying on the numerical method above.

Suppose that a walker starts from a point at $N = 0$. We have then the probability distribution function $Q(0, 0) = 1$ at $N = 0$. This leads to

$$g_{11} = g_{22} = g_{12} = 0, \quad (N = 0). \tag{26}$$

Hence the $N = 0$ manifold does not extend to any direction or it degenerates to a point.

At $N = 1$ the probability functions are given by

$$Q(0,1) = q_1 Q_1(0,0) + q_2 Q_2(0,0), \quad Q(1,1) = p_1 Q_1(0,0) + p_2 Q_2(0,0). \tag{27}$$

The two functions, of course, satisfy the normalization condition $Q(0, 1) + Q(1, 1) = 1$. It is possible to regard one of the two functions as a coordinate transformation, for instance, $\theta_1 = Q(0, 1)$. We then adopt a function independent of $Q(0, 1)$ as θ^2. The new coordinate system produces

$$g_{11} = \frac{1}{\theta^1(1-\theta^1)}, \quad g_{22} = g_{12} = 0, \quad (N = 1). \tag{28}$$

Thus the $N = 1$ manifold has no extension to the θ^2 direction or it degenerates to a line.

At $N = 2$, the degeneration dissolves, and the manifold then turns to a space of constant curvature. We now show the fact. It is very cumbersome and troublesome to explicitly calculate geometrical quantities by using the coordinate system (p_1, q_2) or its linear transformation. It is convenient to choose as a coordinate system any two of the probability functions

$$\begin{aligned} &Q(0,2) = q_1 q_2 Q_1(0,0) + q_2^2 Q_2(0,0), && (a)\\ &Q(1,2) = (q_1 p_2 + p_1 q_1) Q_1(0,0) + (p_2 q_1 + q_2 p_2) Q_2(0,0), && (b)\\ &Q(2,2) = p_1^2 Q_1(0,0) + p_1 p_2 Q_2(0,0). && (c) \end{aligned} \tag{29}$$

For instance, choice of $\theta^1 = Q(1, 2)$ and $\theta^2 = Q(2, 2)$ makes the probabilities reduce to simple expressions:

$$Q(0,2) = 1 - \theta^1 - \theta^2, \quad Q(1,2) = \theta^1, \quad Q(2,2) = \theta^2. \tag{30}$$

These expressions produce the metric components as follows:

$$g_{ij} = E(\partial_i l \partial_j l) = \frac{1}{1-\theta^1-\theta^2} + \frac{1}{\theta^i}\delta_{ij}. \tag{31}$$

And also we have

$$T_{ijk} = E(\partial_i l \partial_j l \partial_k l) = \frac{-1}{(1-\theta^1-\theta^2)^2} + \frac{\delta_i^1 \delta_j^1 \delta_k^1}{(\theta^1)^2} + \frac{\delta_i^2 \delta_j^2 \delta_k^2}{(\theta^2)^2}. \tag{32}$$

Equations (31) and (32) lead to

$$g_{ij,k} = -T_{ijk}, \quad \Gamma^{(0)}_{ijk} = -1/2 T_{ijk} \tag{33}$$

in the coordinate system. If one takes advantage of eq. (33), it is easy to calculate the α-curvature. The calculation yields

$$R_{ijkl} = \frac{1-\alpha^2}{2}\frac{1}{2}(g_{ik}g_{jl} - g_{il}g_{jk}). \tag{34}$$

and also

$$R = \frac{1 - \alpha^2}{2}, \quad R_1 = R_2 = 0. \tag{35}$$

3.4 Riemann curvature for N ≥ 2

In a recent paper (Obata, Hara and Endo 1994b) we analyzed the time development of the Riemann curvature, that is, the α-curvature of $\alpha = 0$. We here review main results.

After $N = 2$, the time development of the Riemann scalar curvature R depends on initial conditions. Figures 3 are results under the initial condition of $Q_1(0, 0) = Q_2(0, 0) = 0.5$. Other initial conditions produced graphs similar to figures 3.

In an early period, $N < 100$, the behavior is complicated. Nevertheless we can find a common feature independent of the initial conditions. The figures suggest that the curvature oscillates in the region $p_1 + q_2 < 1$. We now note that the R in $p_1 + q_2 \ll 1$ violently oscillates and also that its value is large as compared with that in other coordinate values. The oscillation is thought to reflect flip-flop motions of such walkers, because $p_1 + q_2 \ll 1$ is equivalent to $q_1 \to 1$ and $p_2 \to 1$. This means that the smaller the value of $p_1 + q_2$ is made, the more frequently the flip-flop steps occur. The larger curvature in $p_1 + q_2 \to 0$ is due to the fact that the localization of the probability function $Q(X, N)$ around the start site $x = X - Y = 0$ is unstable. In the limit state $(p_1, q_2) \to (0, 0)$, the walker stays forever at $x = 0$ or $x = \pm 1$, while in the other states the walker can diffuse to distant sites. Thus a slight variation around the origin $(p_1, q_2) = (0, 0)$ produces a large change of the probability function. In other words the limit state $(p_1, q_2) \to (0, 0)$ is unstable. Thus the unstableness of the limit state is distinctly reflected by two properties of the statistical manifold: the Riemann scalar curvature near the unstable state is larger than that of the other states and it also oscillates violently.

In an early period, $N < 50$, the curvature of a state around $(p_1, q_2) \sim (1, 1)$ rapidly decreases. For instance, refer to the curve of $(p_1, q_2) = (0.9, 0.7)$. The details depend on initial conditions, but the behavior of rapid decreasing is an universal property. This property can also be understood by interpreting the Riemann scalar curvature as a measure of unstableness. At the start time a walker is localized at a point, $x = 0$. If the walker is specified by $(p_1, q_2) \sim (1, 1)$, it moves quickly out of the origin, as compared with other walkers. Hence its unstable motion near the start time produces a rapid change in the probability function $Q(X, N)$, and conse-

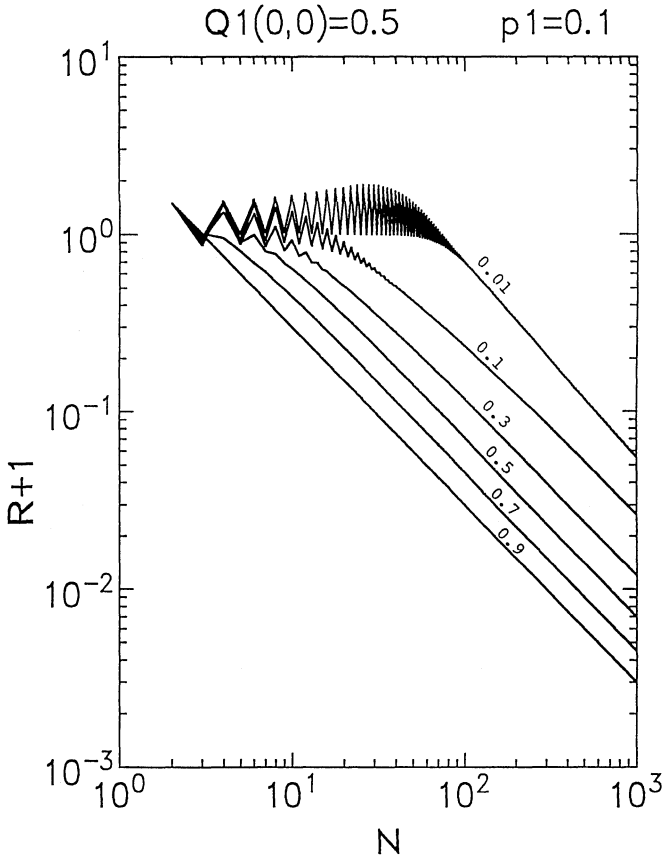

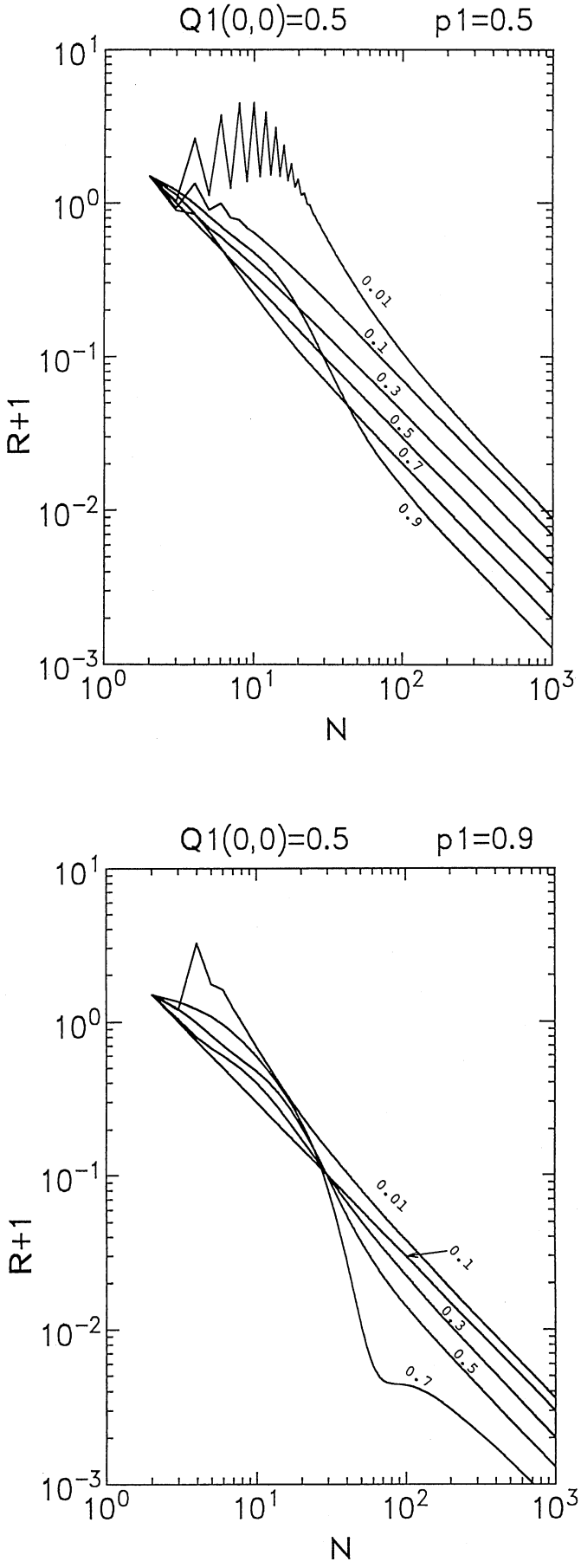

Fig. 3. Time development of the Riemann scalar curvature R plus 1 at some typical coordinate values under an initial condition $Q_1(0, 0) = 0.5$. The coordinate p_1 and the initial condition are indicated at the top of each figure. The coordinate q_2 is shown for each curve.

quently the curvature is expected to vary by a large amount in time.

Thus in early periods the walkers of $(p_1, q_2) \sim (1, 1)$ as well as $(p_1, q_2) \sim (0, 0)$ are unstable and the unstableness appears as the noticeable behavior of the Riemann scalar curvature.

Let us note the asymptotic behavior of $N \to \infty$. Figures 3 suggest

$$R \to -1 + h(p_1, q_2)/N. \tag{36}$$

In order to examine the inhomogeneity $h(p_1, q_2)$ in the order of N^{-1}, we show details of the R at $N = 1000$ in figure 4, using the linear transformation

$$u = (p_1 + q_2)/2, \quad v = (p_1 - q_2)/2. \tag{37}$$

For a fixed u the v varies in the range $-0.5 + |u - 0.5| < v < 0.5 - |u - 0.5|$. The full lines correspond to an initial condition, $Q_1(0, 0) = 1$, and the broken lines to another initial condition, $Q_1(0, 0) = 0.5$. Any broken line of $u < 0.8$ is omitted, because such a line coincides with the full line of the same coordinate value. The other initial conditions also produced similar behavior, so we do not show their curves.

Does the dependence on the initial conditions around $u = 0.9$ at $N = 1000$ mean that the N^{-1} term depends on initial conditions? To answer this question, we calculated the Riemann scalar curvature at later times. Figure 5 shows the curvature in the region $u = 0.9$ at $N = 1000$, 3000, 5000 under two typical initial conditions $Q_1(0, 0) = 1$, 0.5. The full lines, $Q_1(0, 0) = 1$, gradually approach the broken lines, $Q_1(0, 0) = 0.5$. Hence we conclude that the inhomogeneity $h(u, v)$ in the N^{-1} term is

(1) independent of initial conditions;

(2) almost independent of the difference coordinate $v = (p_1 - q_2)/2$, the asymmetry between rightward steps and leftward steps;

(3) monotonically decreasing with respect to another coordinate $u = (p_1 + q_2)/2$, the mean of the diagonal components of the transition probabilities.

Note that the coordinate u represents the orderliness of walks. In fact, $u \to 1$ is equivalent to $p_2 \to 0$ and $q_1 \to 0$, so a walker of $u \sim 1$ tends to walk smoothly and regularly. We may then regard the coordinate u as a 'regularity parameter' or an 'order parameter'. Hence the third property of the inhomogeneity function represents that the Riemann scalar curvature R is small for ordered states in the asymptotic time region.

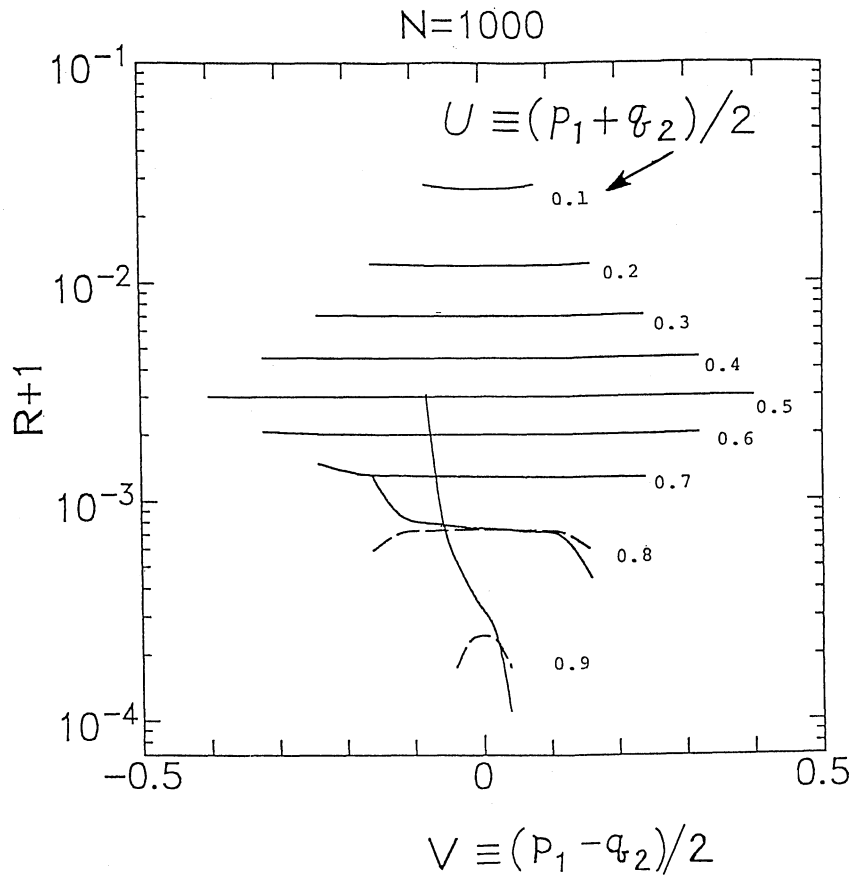

Fig. 4. The right-left asymmetry $(p_1 - q_2)/2$ versus the Riemann scalar curvature R plus 1 at $N = 1000$ for various values of $(p_1 + q_2)/2$. The full lines correspond to $Q_1(0, 0) = 1$, and the broken lines to $Q_1(0, 0) = 0.5$.

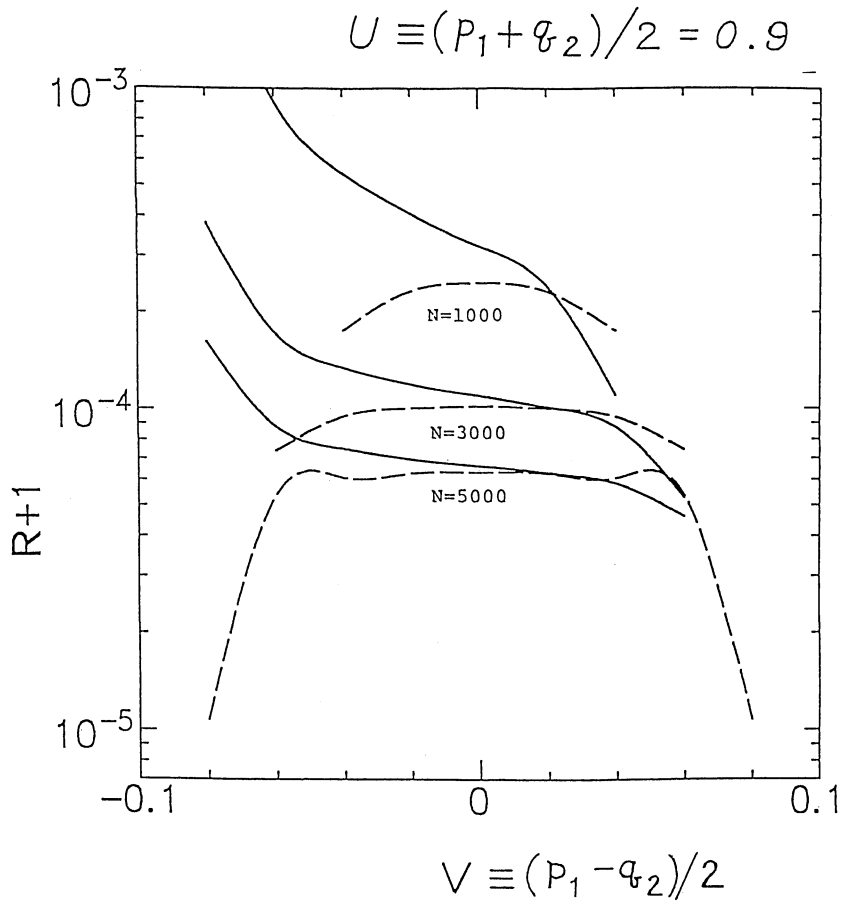

Fig. 5. The right-left asymmetry $(p_1 - q_2)/2$ versus the Riemann scalar curvature R plus 1 at $N = 1000$, 3000 and 5000 for $(p_1 + q_2)/2 = 0.9$. The full lines correspond to $Q_1(0, 0) = 1$, and the broken lines to $Q_1(0, 0) = 0.5$.

3.5 $\alpha(=1)$-curvature for $N \geq 2$

We have seen in section 2 that the 2-dimensional α-curvature tensor can be decomposed into three curvature scalars R_1, R_2 and R. Let us now examine the time development of the curvature scalars in the case of $\alpha = 1$.

As for the CW manifold, there is a symmetry between R_1 and R_2;

$$R_1(p_1, q_2)|_{(a,b)} = R_2(p_1, q_2)|_{(b,a)}. \tag{38}$$

We have ascertained this relation through the numerical calculation of double precision at 5×5 points $(p_1, q_2) \in N_5 \times N_5$, $N_5 \equiv \{0.1, 0.3, 0.5, 0.7, 0.9\}$, each step in $N \leq 100$, every 100 steps in $100 \leq N \leq 1000$, every 1000 steps in $1000 \leq N \leq 5000$. The numerical calculation at many sites and many steps suggests that the symmetry is independent of sites and steps. We should note that the symmetry is inherent in the coordinate system (p_1, q_2). In other words, the coordinate system is a preferred coordinate system in the CW manifold.

Figures 6 show the time development of R and R_1 at some sites in the preferred coordinate system. The R_2 can be read by using the symmetry (38). The full lines stand for $+R$ and the broken lines do for $-R$.

In the asymptotic region, R_2 monotonically decreases and converges to zero. So R_1 behaves in the same way. However, the R monotonically decreases in a region and increases in another region. Thus it is difficult to interpret the nonRiemannian scalar curvature R as a measure of unstability.

We should note a characteristic of the nonRiemann curvature scalars;

$$R, \quad R_1, \quad R_2 \to 0, \quad (N \to \infty). \tag{39}$$

This is equivalent to

$$R^{(1)}_{ijkl} \to 0, \quad (N \to \infty). \tag{40}$$

Therefore we can conclude that the CW manifold is flat in $N \to \infty$ in the meaning of $\alpha = 1$.

The $\alpha = 1$ flatness is the same characteristic as the statistical manifold associated with any equilibrium thermodynamical system, whose distribution function belongs to the exponential family. The exponential family is known to be flat at $\alpha = 1$ (Amari (1985)). Some examples of $\alpha = 1$ flat and homogeneous manifolds are known;

$R^{(0)} = -1$ for normal distributions $N(\mu, \sigma)$ and $R^{(0)} = 0$ for classical ideal gases. Their probability functions belong to the exponential family. We showed $R^{(0)} \to -1$ for the CW manifold. Comparing the CW manifold with the geometry of $N(\mu, \sigma)$, we might guess that the distribution functions of the CW manifold approach to the normal distributions. However, the guess seems to be wrong, because $Q(X, N)$ is known to have a sharp peak, called the runaway component (Fujita (1986)), at $X \sim N$ for $p_1 \sim 1$, $p_2 \sim 1$ under the initial condition $Q_1(0, 0) = 1$ and $Q_2(0, 0) = 0$.

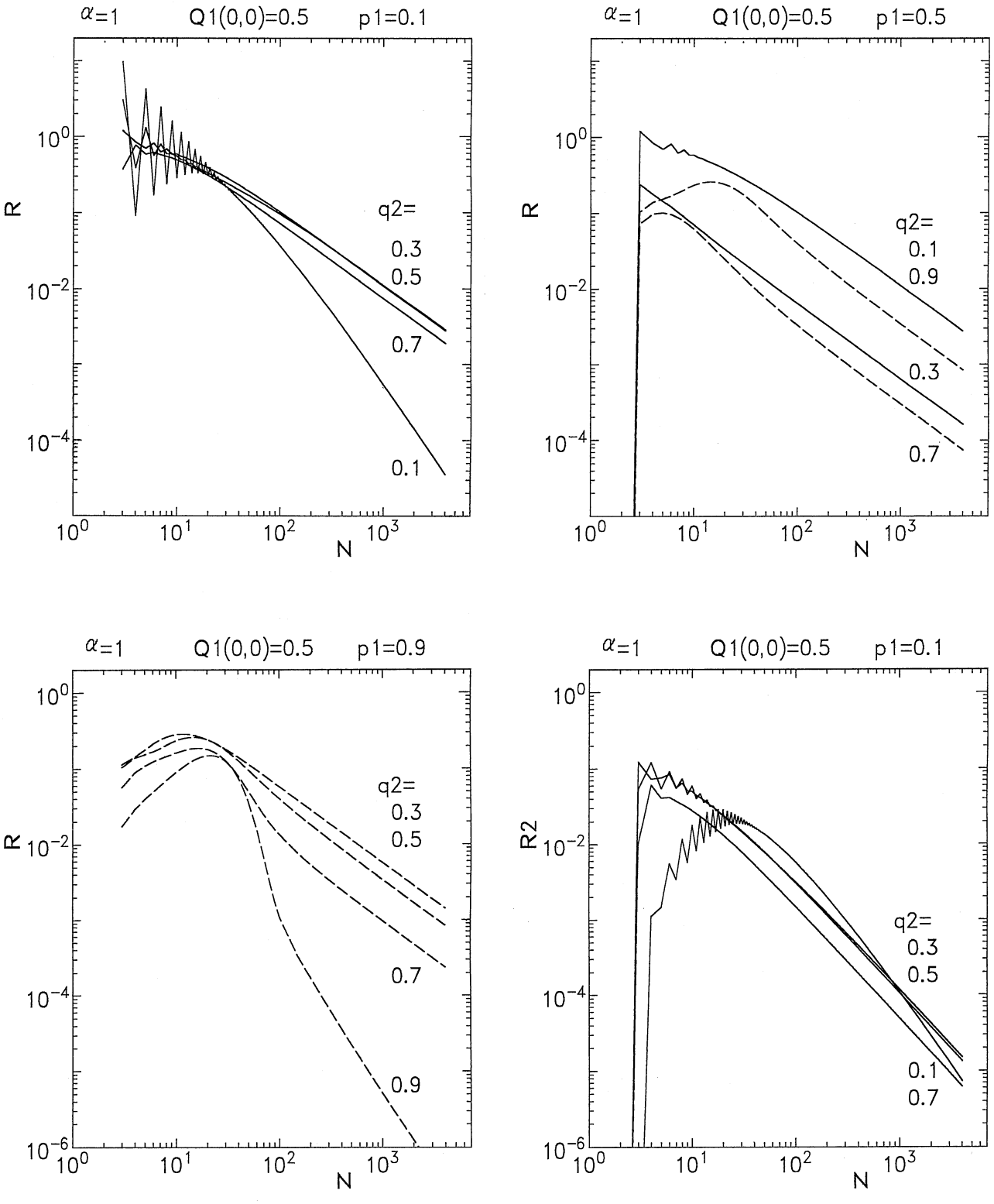

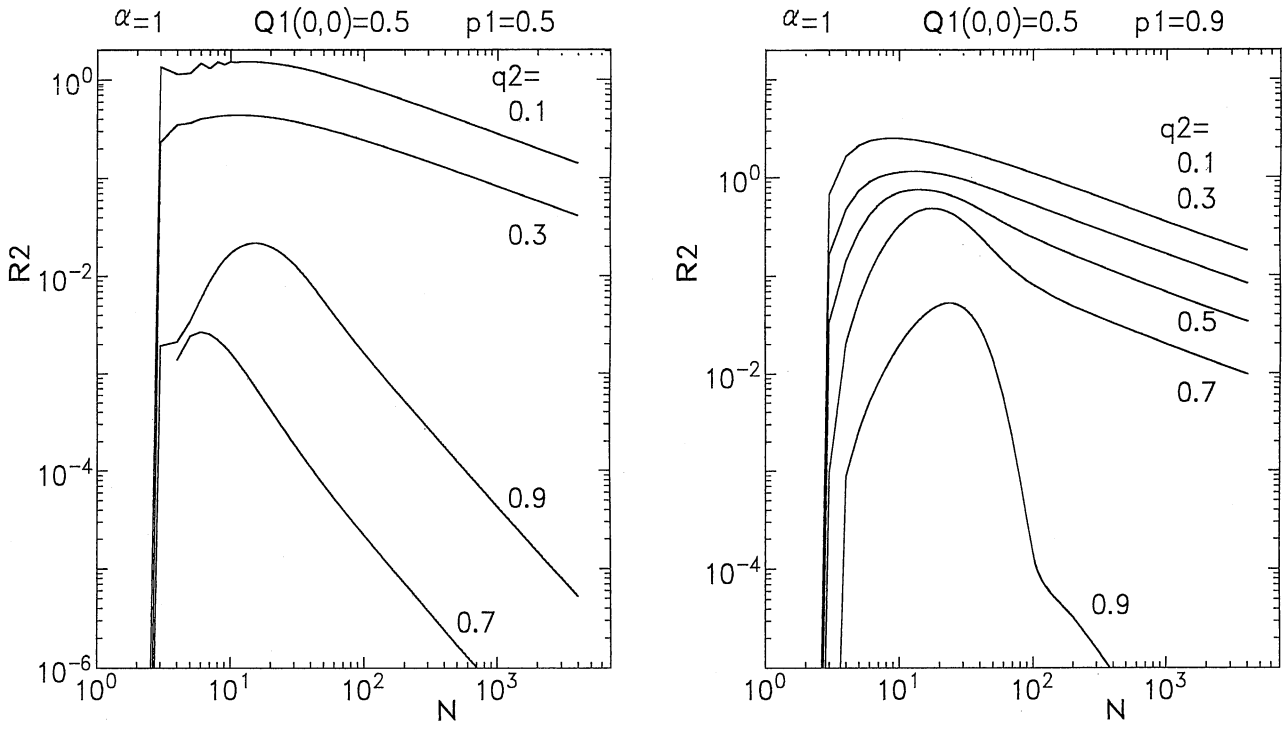

Fig. 6. Time development of the $\alpha(=1)$-curvature invariants R and R_2 at some typical coordinate values under an initial condition $Q_1(0, 0) = 0.5$. The coordinate p_1 and the initial condition are indicated at the top of each figure. The coordinate q_2 is shown for each curve. The full lines are for $+R$ and $+R_2$, and the broken lines for $-R$ and $-R_2$.

4 Perspectives

4.1 A prediction to n-step correlation walks

The Riemann scalar curvature of the D-dimensional RW statistical manifold approaches to (2D-1)D/N for large step number N (Obata, Hara and Endo (1992)). In the CW model with the correlation of successive two steps, the asymptotic form of the Riemann scalar curvature is given by eq. (36). Upon these results we now infer the asymptotic behavior of the Riemann scalar curvature about CW models with the correlation of successive n steps. If successive steps are strongly correlated, the motion will be orderly. Hence if the Riemann scalar curvature is a measure of unstability, we can expect that the Riemann scalar curvature has the asymptotic form of

$$R^{(0)} \to -C_{\#} + h/N. \tag{41}$$

The $C_{\#}$ is inferred to be a monotonically decreasing function in the number n of correlated steps. And also the manifold is anticipated to be asymptotically $\alpha(=1)$-flat.

4.2 Generalized models

The CW model in section 3 and its generalizations to n-step correlation walks are described in terms of linear equations with constant coefficients. There are many further generalized models in literature. For instance, Hara et al. introduced memory functions in random walk processes (Hara (1979), Hara, Choi and Chung (1987), Hara, Obata and Lee (1988)). Then the time development equations for probability functions turn out to be nonlinear. They discussed the fluctuation and bifurcation of paths in the generalized models.

If the Riemann scalar curvature is a general measure of unstability, we might expect the curvature to be useful also in discussing the fluctuation and bifurcation of paths. And also we might obtain some geometrical characteristics about parameters of the models by examining the α-curvarue.

One should note that the method of numerical analysis discussed in section 3.2 applies to nonlinear equations as well as linear equations.

4.3 Newton-Cartan-like geometrical structure

The time development of a nonequilibrium process leads to a stack of statistical manifolds parameterized by a discrete time or a continuous time. This stack should be called to be a stratified space. Each layer, of course, has the geometrical structure of a statistical manifold. In addition we note that different layers have relation to each

other. Because the time development equations for probability functions relate a point at a layer, that is, a probability function to a point at a neighboring layer.

We should remark that this structure is remarkably analogous to the Newton-Cartan theory of gravity (Misner, Thorne and Wheeler (1973), Trautman (1965)). To see it, we review the gravitational theory in brief.

In Newton dynamics, the equation of motion for a test particle

$$\frac{d^2x^j}{dt^2} + \frac{\partial \Phi}{\partial x^j} = 0 \tag{42}$$

is usually interpreted as an equation of describing curved paths in Euclid space. Newton-Cartan theory regards the equation of motion as an equation defining geodesics $[t(\lambda), x^j(\lambda)]$ in a curved space. The clock carried by a test particle ticks an universal time t (or a constant multiplication $\lambda = at + b$). So we can rewrite the equation of motion as

$$\frac{d^2t}{d\lambda^2} = 0, \quad \frac{d^2x^j}{d\lambda^2} + \frac{\partial \Phi}{\partial x^j}\left(\frac{dt}{d\lambda}\right)^2 = 0. \tag{43}$$

As compared with the equation of geodesic, we can read the connection coefficients

$$\Gamma^j_{00} = \frac{\partial \Phi}{\partial x^j}, \quad \textit{the other components} = 0. \tag{44}$$

The connection coefficients yield the affine curvature tensor

$$R^j_{0k0} = \frac{\partial^2 \Phi}{\partial x^j \partial x^k}, \quad \textit{the other components} = 0. \tag{45}$$

The Ricci tensor $R_{\alpha\beta}$ $(\equiv R^{\mu}_{\alpha\mu\beta})$ is then

$$R_{00} = \Delta \Phi. \tag{46}$$

Hence the equation for Newton potential Φ can be transformed into a spacetime equation,

$$R_{00} = 4\pi G\rho. \tag{47}$$

The short review shows that the fundamental geometrical structure of Newton-Cartan spacetime is characterized by the universal time, the connection given by the equation of motion and the 3-dimensional Euclid metric. One should note that the metric is not a spacetime metric but a space metric. As compared with the statistical manifold of correlated walks, we can read the following correspondence.

Newton-Cartan theory	CW statistical manifold
universal time t	step time N
equation of motion for a test particle	time development equation for probability functions
3-dimensional Euclid metric	information matrix ($+\alpha$ curvature)

The equation of motion for a test particle produces an affine connection in the Newton-Cartan spacetime. So we expect from the correspondence table that the time development equation for probability functions produces a geometrical object in the stacked statistical manifold. However, it is not straightforward to read the geometrical object from the correspondence, because a point in the statistical manifold and the stacked statistical manifold is a probability function. And also the time development equation for the probability function is not a differential equation of 2nd rank but a difference equation of 1st rank.

What are geometrical objects produced by the time development equation for probability functions?

REFERENCES

[1] Amari, S., (1985), "Differential-Geometrical Methods in Statistics (Lecture Notes in Statistics 21)", (Springer, Berlin).

[2] Fujita, S., (1986), "Statistical and thermal physics part I. Probabilities and Statistics, Thermodynamics and Classical Statistical Mechanics", (Krieger: Malabar, FL), pp39–56, 467–471.

[3] Fujiwara, A. and Amari, S., (1993), "Dualistic Dynamical Systems in the Framework of Information Geometry", METR93-17, Univ. Tokyo, 1-23.

[4] Ginoza, M.,(1993), "RIEMANNIAN GEOMETRY OF EQUILIBRIUM THERMO-DYNAMICS IN A LIQUID MIXTURE", Rep. Math. Phys. 32, 167–174.

[5] Hara, H., (1979), "Generalization of random-walk process", Phys. Rev. B. 20, 4062–4098.

[6] Hara, H., Choi, S. D., and Chung, C., (1987), "A THEORY OF NOISE BASED ON GENERALIZED RANDOM WALKS", Physica A 144, 481–494.

[7] Hara, H., Obata, T., and Lee, S. J., (1988), "Fluctuations and bifurcations of the paths described by generalized ran-

dom walks", Phys. Rev. B 37, 476–486.
[8] Janyszek, H., (1986), "On the Riemannian metrical structure in the classical statistical equilibrium thermodynamics", Rep. Math. Phys. 24, 1–10.
[9] Janyszek, H., (1990), "Riemann geometry and stability of thermodynamical equilibirium systems", J. Phys. A: Math. Gen. 23, 477–490.
[10] Janyszek, H. and Mrugala, R., (1989), "Riemann geometry and the thermodynamics of model magnetic systems", Phys. Rev. A 39, 6515–6523.
[11] Janyszek, H. and Mrugala, R., (1990), "Riemann geometry and stability of ideal quantum gases", J. Phys. A: Math. Gen. 2, 467–476.
[12] Misner, C. W., Thorne, K. S., and Wheeler, J. A., (1973), "GRAVITATION", (Freeman, San Francisco), Chapter 12.
[13] Nakamura, Y., (1993), "Completely integrable gradient systems on the manifolds of Gaussian and multicomponent distributions", Jap. J. Industrial and Appl. Math. 10, 179.
[14] Obata, T., Hara, H., and Endo, K., (1992), "Differential geometry of nonequilibrium processes", Phys. Rev. A 45, 6997–7001.
[15] Obata, T., Hara, H., and Endo, K., (1994), "Dynamical behaviour of a statistical manifold associated with correlated walks", J. Phys. A: Math. Gen. 27, 5715–5726.
[16] Obata, T., Hara, H., and Endo, K., (1994), "Dynamics of Correlated Walks from the Viewpoint of Differential Geometry", Proc. Int. Conf. on STATISTICS IN INDUSTRY, SCIENCE AND TECHNOLOGY, 96–101.
[17] Ruppeiner, G., (1979), "Thermodynamics: A Riemannian geometrical model", Phys. Rev. A 20, 1608–1613.
[18] Ruppeiner, G., (1995), "Riemannian geometry in thermodynamic fluctuation theory", Rev. Mod. Phys. 67, 605–659.
[19] Ruppeiner, G. and Davis, C., (1990), "Thermodynamic curvature of the multicomponent ideal gase", Phys. Rev. A 41, 2200.
[20] Trautman, A., (1965), "Foundations and Current Problems of General Relativity, (Lectures on General Relativity, Brandeis 1964 Summer Institute on Theoretical Physics, vol. I)", (Prentice-Hall, N.J.).